Alexandria Engineering Journal (2016) 55, 2583–2588

HOSTED BY
ELSEVIER

Alexandria University

Alexandria Engineering Journal

www.elsevier.com/locate/aej
www.sciencedirect.com

ORIGINAL ARTICLE

Segmentation of lung nodule in CT data using active contour model and Fuzzy C-mean clustering

Ezhil E. Nithila *, **S.S. Kumar**

Noorul Islam Centre for Higher Education, Kumaracoil 629180, India

Received 24 November 2015; revised 25 March 2016; accepted 4 June 2016
Available online 14 June 2016

KEYWORDS

Active contour;
Segmentation;
FCM;
Error rate;
Similarity measure

Abstract The aim of this paper was to develop a region based active contour model and Fuzzy C-Means (FCM) technique for segmentation of lung nodules. Ultimately, detection and assisted diagnosis of nodules at earlier stage increase the mortality rate. Among many imaging modalities, Computed Tomography (CT) is being the most sought because of its imaging sensitivity, high resolution and isotropic acquisition in locating the lung lesions. The proposed methodology focuses on acquisition of CT images, reconstruction of lung parenchyma and segmentation of lung nodules. Reconstruction of parenchyma can be employed using selective binary and Gaussian filtering with new signed pressure force function (SBGF-new SPF) and clustering technique was used for nodule segmentation. Comparative experiments demonstrate the advantages of the proposed method in terms of decreased error rate and increased similarity measure.

1. Introduction

Of the other cancers (colon, breast and prostate cancer), the most serious death causing cancer is Lung cancer. Recently, the United States has diagnosed 2,28,190 peoples with lung cancer [1]. Most of the people were diagnosed with lung cancer having non-small cell lung cancer rather small cell lung cancer. Early diagnosis and diagnosis are important for the increase in survival rate up to 50% [2].

Nodule identification is one of the fundamental problems in medical image processing. Pulmonary nodules are small tissue in the lung and most of them are benign [3]. To assist the specialist, with the information regarding nodules in lung parenchyma computer-aided detection (CAD) system was developed. An automated CAD system was designed to detect the nodule sized between 3 and 30 mm. CAD has more advantages in terms of speed, accuracy [4], detection of nodules in pulmonary CT images and a reduction in miss rate [5,6]. Segmentation is an essential step in many applications involving CAD. It partitions the image into segments corresponding to the anatomical objects in the image. In the recent years, a lot of pulmonary nodule segmentation methods have been proposed, which can be categorized as thresholding method [7,8], morphological method [9], deformable model [10], clustering method [11–13], graph cut method [14,15], Markov random field, region growing [16], watershed, neural networks, fuzzy logic, active contours [17] and histogram based segmentation [18].

Among various segmentation methods, active contour was one of the most popular and successful one. Many researchers are devoted to study the detection of pulmonary nodules

* Corresponding author.
E-mail address: ezhilniche@gmail.com (E.E. Nithila).

Peer review under responsibility of Faculty of Engineering, Alexandria University.

http://dx.doi.org/10.1016/j.aej.2016.06.002
1110-0168 © 2016 Faculty of Engineering, Alexandria University. Production and hosting by Elsevier B.V.

attached to vessels and the pulmonary wall. El-Bazl et al. [19] proposed a segmentation technique using Markov random field, consisting of two stages. The first stage is to select the optimum decision level to create an initial labeling image, and the second one is to extract the lung tissues from each slice. Using this methodology, about 50 subjects were evaluated. Out of this 40 subjects were normal and ten subjects had abnormalities in their CT scans.

Tong et al. [20] used a three step process to detect lung nodules. Firstly, an adaptive threshold algorithm was used to segment the lung region. Secondly, active contour model (ACM) was used to remove lung vessel and finally a Hessian matrix (selective shape filter) was used to detect the suspicious nodules. This method was able to produce an overall detection rate of 85%. Marten et al. [21] evaluated and compared features such as nodule size, position, margin, matrix characteristics, vascular and pleural attachments with gold standard. Some authors use manually segmented lesion as the gold standard and some other uses specialist references as the gold standard. Azimifar et al. [22] used active contour modeling for segmentation and produces an overall detection rate of 89%. Dehmeshki et al. [23] proposed volumetric measurement for the detection of lung nodule. A new region growing method for segmentation in combination of fuzzy connectivity, distance and intensity information as the growing mechanism and peripheral contrast as the halting criterion has been used. It was found that this method is highly reproducible for various types of nodules from various data protocols. All these works aim to detect lung nodule automatically from CT images.

Most of them produce segmentation results with less accuracy which is undesirable for clinical usage. Hence it is necessary to develop a suitable technique which segments lung nodules with good accuracy, reduced computation time and less segmentation error rate per image.

The present work aims to segment the lesion automatically with the help of CT images. For lung reconstruction, Selective Binary and Gaussian Filtering with new signed pressure force function (SBGF-new SPF) and segmentation of lung nodule, 3-class FCM was used.

2. Methodology

Automatic nodule detecting scheme using CT scans helps the physicians to reduce the load and to improve detection quality. The methods proposed for the detection of lung nodule consist of the CT lung acquisition and the segmentation of lung nodules. The main aim of this process was to remove the portions that are part of the CT image other than lung lesion. Fig. 1 shows the various stages of segmentation scheme.

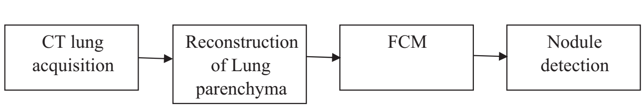

Figure 1 Main diagram of segmentation scheme.

2.1. CT lung acquisition

The Lung Image Database Consortium image collection (LIDC-IDRI) consists of diagnosing and lung cancer screening thoracic CT scans with marked-up annotated lesions [24]. It is a web-accessible resource for development, training, and evaluation of CAD methods for lung cancer detection and diagnosis.

2.2. Reconstruction of lung parenchyma

The objective of this stage was to eliminate the mediastinum and thoracic wall and to separate the parenchyma using region based ACM. There exist many region based models such as Geodesic active contour (GAC) model [25], Chan–Vese (C–V) model [26], Piecewise Smooth (PS) model [27], Local Binary Fitting (LBF) [28] model and so on. Some models suffer due to weak edges and others due to evolutionary time. But SBGF-new SPF performs well under weak edges, with less computational time and increased efficiency.

2.2.1. The proposed method

Based on the work inspired by [29] the proposed method segments the lung nodule and has the advantage of easy implementation, speed, less segmentation error and accuracy.

In order to increase the efficiency, the algorithm was modified by the inclusion of contour constants in SPF function. Let $\Omega \in R^3$ be the image domain, and $I(x)$ be the input image. Let c_1, c_2 be the constants inside and outside the contour. The proposed method uses selective step and no re-Initialization is required. It first penalizes level set function to be binary, and then uses a Gaussian filter to regularize it. The Gaussian filter can make the level set function smooth and the evolution more stable. The balloon force α is used for shrinking or expanding the contour. The Signed Pressure Force (SPF) function is used to control the direction of evolution. The function ranges in $\{-1, 1\}$. It uses local image information. It modulates the signs of the pressure force which shrinks of contour inside the object and expands of contour outside the object. A Gaussian kernel is used to regularize the level set function which not only regularizes it but also removes the need of computationally expensive re-initialization. If the object boundary has gaps, the contour tends to leak and hence boundary leakage problem arises. This can be solved by applying an edge stopping function, which pulls the contour to the boundary [30]. The existing methodology uses more iteration. The proposed methodology does not change the functionality of evolution but reduces the number of iterations.

Therefore, the energy function of the proposed system was given by

$$\frac{\partial \phi}{\partial t} = c_1 * c_2 * spf(I(x)) * \alpha|\nabla \phi|, \; x \in \Omega \tag{1}$$

$$spf(I(x)) = \frac{I(x) - \frac{c_1+c_2}{2}}{\max\left(\left|I(x) - \frac{c_1+c_2}{2}\right|\right)}, \; x \in \Omega \tag{2}$$

$$c_1(\phi) = \frac{\int_\Omega I(x) * H(\phi)dx}{\int_\Omega H(\phi)dx} \tag{3}$$

$$c_2(\phi) = \frac{\int_\Omega I(x) * (1 - H(\phi))dx}{\int_\Omega (1 - H(\phi))dx} \tag{4}$$

Using Eq. (1) the energy function can be formulated. The parameters such as sigma (σ), number of iterations, delta and alpha (α) can be varied to obtain the desired lung parenchyma. Decreasing σ results in incomplete lung lobe. On the other hand increasing σ results in large time consumption.

2.2.2. Reconstruction of lung border

The reconstruction of the lung border is an important step that aims to recover lung nodules that are attached to the thoracic wall. The juxtapleural nodule can be recovered using Adaptive border marching [31], greedy snake algorithm [32], ray casting, vector quantization [33], and chain codes [34]. The present work employs a technique called rolling ball, which uses morphological closing operations with a circular structuring elemental along the contour of the lung, causing the reconstruction of the concavities where this element cannot enter. The structuring element was used in a disk with radius equal to 12.

2.3. FCM

Clustering algorithms achieve region segmentation by partitioning the image into sets or clusters of pixels that have strong similarity in the feature space. In hard clustering, data are divided into distinct clusters, where each data element belongs to exactly one cluster. In fuzzy clustering, data elements can belong to more than one cluster, and associated with each element is a set of membership levels. These indicate the strength of the association between that data element and a particular cluster [35,36].

Fuzzy clustering is a process of assigning these membership levels, and then using them to assign data elements to one or more clusters. One of the most widely used fuzzy clustering algorithms is the FCM Algorithm [37]. This can be used in many fields such as pattern recognition, fuzzy identification, and feature extraction.

Let $U \in M_{fc}$ be a fuzzy c partition of X, and the FCM function [42] is defined as

$$J_m(U,v) = \sum_{k=1}^{n}\sum_{i=1}^{c}(u_{ik})^m (d_{ik})^2$$
$$d_{ik}^2 = \|x_k - v_i\|^2 \tag{5}$$

The FCM algorithm produces a fuzzy c partition of the data set $X = \{x_1, x_2, \ldots x_n\}$. The 3-class FCM algorithm is used to segment the region of interest from the reconstructed lung. The region of interest (ROI) contains nodules, blood vessels and bronchi. In order to separate nodule from these structures, morphological operations are performed.

3. Results and discussion

The proposed system uses LIDC for the evaluation on lung CT. For benignity the nodule size is 3–30 mm and >30 mm for malignancy. The original lung CT, reconstructed lung parenchyma, FCM output and segmented nodule detection output for different candidates are shown in Fig. 2. It has been found that the segmented output can be achieved at faster rate with less number of iterations. The number of iterations required is 140 with a response time of less than 1 min. The parameters are used in the proposed algorithm for separating the parenchyma from the mediastinum and the thoracic wall and nodule detection are σ equal to 0.3, 1 and 2, number of iterations to segment is equal to 150, delta equal to 1, $\propto$ equal to 4 and number of clusters is equal to 3. It was noted that if the size of parenchyma is large, the number of iterations can changed to higher value. No other parameter needs to be changed.

3.1. Quantitative metrics for evaluation

The images that are segmented manually are termed as Gold Standard (GS). S denotes the automated segmented image. Let e_i be the error measure and n be the number of samples used. Evaluation of segmented (S) against GS images was made for following measures:

a) Volume error, $VE = \dfrac{2(S - GS)}{(S + GS)}$ (6)

b) Coefficient of Similarity $= 1 + \dfrac{(GS \cap S)}{GS}$ (7)

c) Spatial overlap $= \dfrac{2(GS \cap S)}{(S \cup GS)}$ (8)

d) RMSE $= \sqrt{\left(\dfrac{1}{n}\right)\sum_{i=1}^{n} e_i^2}$ (9)

e) Under segmentation rate, $U = |GS - (S \cap GS)|$ (10)

f) Over segmentation rate, $V = |S - (S \cap GS)|$ (11)

The average volume error is 0.968%. For clinical usages, less than 5% volume error is more likely suitable [38]. Figs. 3 and 4, show the comparison of coefficient of similarity and spatial overlap between LBF and proposed method. Coefficient of similarity shows the resemblances between the segmented and gold standard images. Spatial overlap is the accurate measure of spatial properties of segmented images. The best coefficient of similarity and overlap fraction is 0.914 and 0.584 and worst is 0.074 and 0.089. According to [41] the spatial overlap of LIDC database can be reported from 0.51 to 0.66. The proposed work shows a spatial overlap fraction of 0.584 which lies within the specified range. Experimental results show that the proposed method shows increased performance when compared with LBF model. In the previous literature Paik et al. [31] suggested an average over segmentation and under segmentation ratio was 0.43% and 1.63%. In the present study, the observed results (average over segmentation and under segmentation ratio) were 0.63% and 0.015% respectively. It was found that the proposed methodology shows better performance when compared with the previous literature results [31].

Table 1 depicts the comparison of various segmentation methods with the proposed method. The root mean square error (RMSE) and overlap measure describe the similarities between segmented and gold standard image. The proposed method achieves RMSE of 0.10 mm and accuracy measure of 98.95%. In research studies the performance of RMSE has been used as a standard statistical metric. The proposed method shows very less error rate when compared with other methods. Under segmentation rate defines the proportion of the unsegmented lesion area. Over segmentation rate is defined as the ratio of the segmented non-lesion area. Figs. 5 and 6

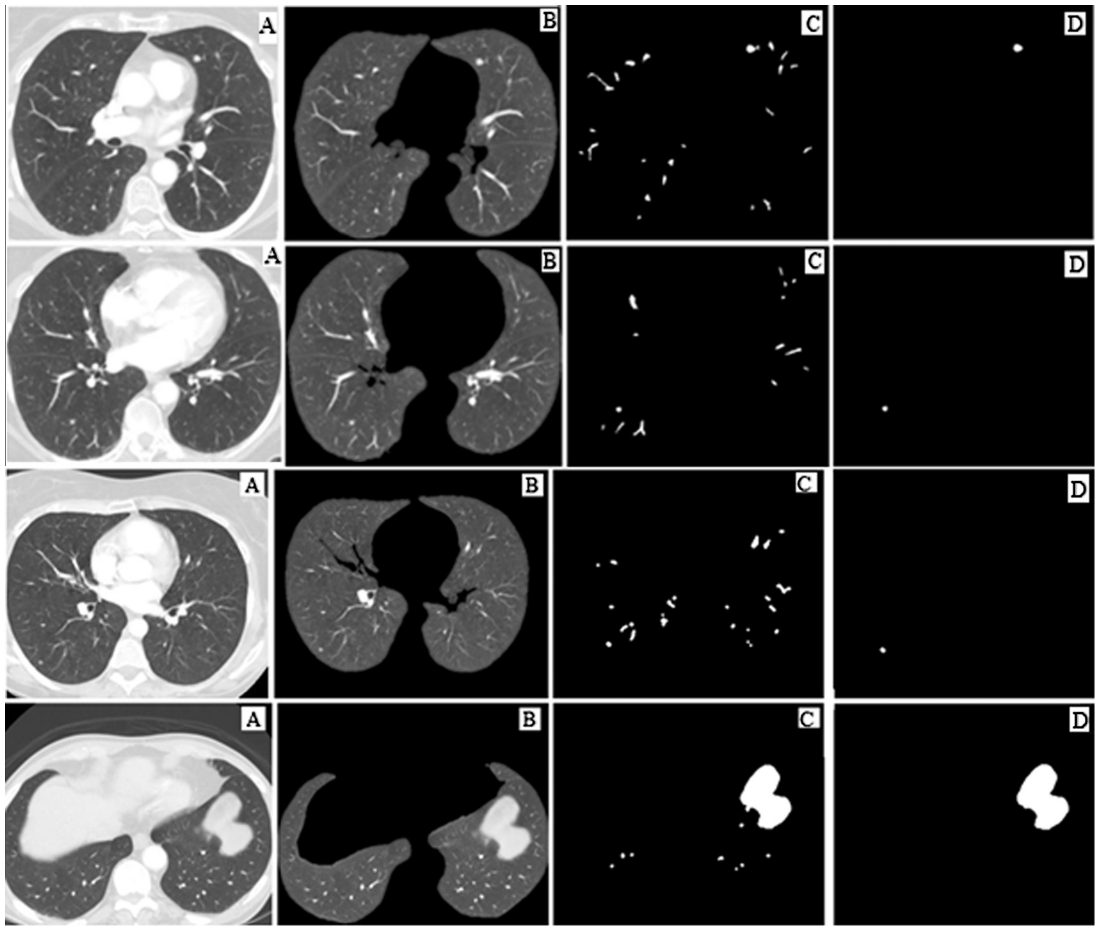

Figure 2 Result of different subjects, (A) Original image, (B) Reconstructed lung, (C) FCM output, (D) Nodule detection.

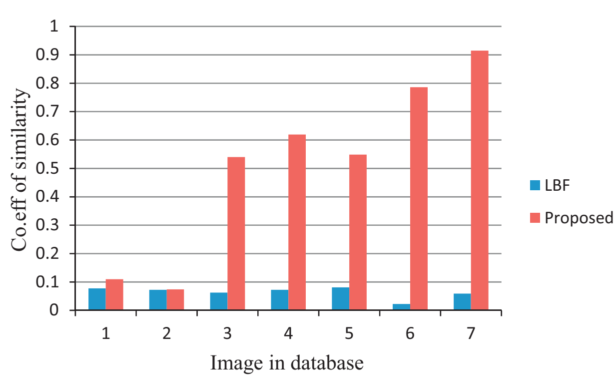

Figure 3 Comparison of coefficient of similarity between LBF and proposed method.

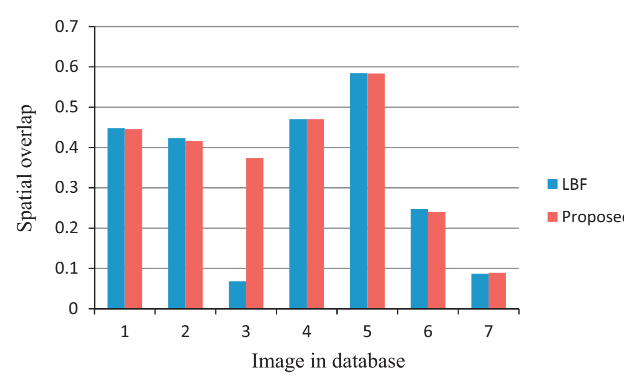

Figure 4 Spatial overlap between LBF and proposed method.

show the over segmentation and under segmentation ratio for LBF and proposed model. The average over segmentation and under segmentation ratio was 0.63% and 0.015% respectively.

3.2. Advantage of proposed model over the LBF model

Compared with LBF, proposed model utilizes global segmentation with less number of iterations and low computation time. LBF uses local segmentation, with more iteration and very high computation time. LBF is a region based active contour model which uses signed distance function (SDF) and requires re-initialization. Evolution converges at 100 iterations with the required time of 454 s whereas the proposed model utilizes 140 iterations for 18 s. The best similarity and overlap fraction are 0.914 and 0.584 and worst is 0.074 and 0.089. The average over segmentation and under segmentation ratio was 0.63% and 0.015% respectively.

Table 1 Performance comparison with other models.

Study	Method	Performance
Hu et al., [39]	Iterative threshold, Morphological Operations	Root mean square Difference = 0.54 mm
Yim et al., [40]	Region growing, Connected component	Root mean square Difference = 0.32 mm
Badura et al. [41]	Modified relative Fuzzy connectedness	Spatial Overlap = 0.6
Deep et al. [42]	Rotation invariant LBP	Accuracy = 98%
Proposed method	SBGF-new SPF, FCM	Root mean square Difference = 0.10 mm Spatial Overlap = 0.584 Accuracy = 98.95%

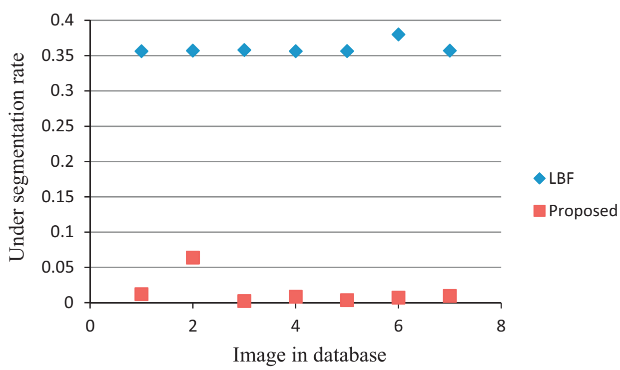

Figure 5 Under segmentation rate of various images in databases.

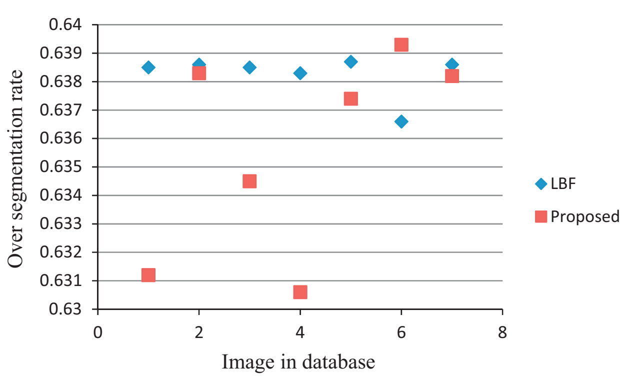

Figure 6 Over segmentation rate of various images.

4. Conclusion

Computer-aided diagnosis of lung cancer is used to segment pathologically changed tissues fast and accurately. The proposed algorithm SBGF-new SPF and FCM successfully segment the lung nodule from the CT. For lesion the average volume error obtained is 0.968%. The coefficients of similarity, spatial overlap, RMSE, average over and under segmentation ratio are 0.914, 0.584, 0.10 mm, 0.63% and 0.015% respectively. The experimental results indicate that the newly proposed algorithm could segment blood vessel adhesion, pleura adhesion fast and exactly performs better than traditional segmentation effects, with executive efficiencies and decreased rate of errors.

Acknowledgment

We express our sincere thanks to DST, New Delhi for the financial support under INSPIRE fellowship scheme for the above research work.

References

[1] American Cancer Society. Cancer Facts & Figures, 2015.

[2] Sheng Chen, Kenji Suzuki, Heber MacMahon, Development and evaluation of a computer-aided diagnostic scheme for lung nodule detection in chest radiographs by means of two-stage nodule enhancement with support vector classification, Med. Phys. 38 (2011) 1844–1858.

[3] K. Alexander, H. Joly, L. Blond, et al, A comparison of computed tomography, computed radiography, and film-screen radiography for the detection of canine pulmonary nodules, Veter. Radiol. Ultrasound 53 (3) (2012) 258–265.

[4] K. Bhavanishankar, M.V. Sudhamani, Techniques for detection of solitary Pulmonary nodules in human Lung and their classifications – a survey, Int. J. Cybernetics Inf. 4 (1) (2015).

[5] W.J. Choi, T.S. Choi, Genetic programming-based feature transform and classification for the automatic detection of pulmonary nodules on computed tomography images, Inf. Sci. 212 (2012) 57–78.

[6] S.C. Park, B.E. Chapman, B. Zheng, A multistage approach to improve performance of computer-aided detection of pulmonary embolisms depicted on CT Images: preliminary investigation, IEEE Trans. Biomed. Eng. 58 (6) (2011) 1519–1527.

[7] A.P. Reeves, A.B. Chan, D.F. Yankelevitz, C.I. Henschke, B. Kressler, W.J. Kostis, On measuring the change in size of pulmonary nodules, IEEE Trans. Med. Imaging 25 (4) (2006) 435–450.

[8] S. Magalhães Barros Netto, A. Corrêa Silva, R. AcatauassúNunes, M. Gattass, Automatic segmentation of lung nodules with growing neural gas and support vector machine, Comput. Biol. Med. 42 (11) (2012) 1110–1121.

[9] F. Dong, J. Peng, Brain MR image segmentation based on local Gaussian mixture model and nonlocal spatial regularization, J. Visual. Comm. Image Rep. 25 (5) (2014) 827–839.

[10] C. McIntosh, G. Hamarneh, Medial-based deformable models in nonconvex shape-spaces for medical image segmentation, IEEE Trans. Med. Imaging 31 (1) (2012) 33–50.

[11] K. Murphy, B. Van Ginneken, A.M.R. Schilham, B.J. de Hoop, H.A. Gietema, M. Prokop, A large-scale evaluation of

automatic pulmonary nodule detection in chest CT using local image features and k-nearest-neighbour classification, MedImage Analysis 13 (5) (2009) 757–770.
[12] A. Ortiz, J.M. Gorriz, J. Ramirez, D. Salas-Gonzalez, Improving MR brain image segmentation using self-organising maps and entropy-gradient clustering, Inf. Sci. 262 (2014) 117–136.
[13] X. Zhang, C. Zhang, W. Tang, Z. Wei, Medical image segmentation using improved FCM, Sci. China Inf. Sci. 55 (5) (2012) 1052–1061.
[14] Y. Boykov, G. Funka-Lea, Graph cuts and efficient N-D image segmentation, Int. J. Comput. Vision 70 (2) (2006) 109–131.
[15] X. Chen, J.K. Udupa, U. Bagci, Y. Zhuge, J. Yao, Medical image segmentation by combining graph cuts and oriented active appearance models, IEEE Trans. Image Process. 21 (4) (2012) 2035–2046.
[16] R. Bellotti, F. De Carlo, G. Gargano, S. Tangaro, A CAD system for nodule detection in low-dose lung CTs based on region growing and a new active contour model, Med. Phys. 34 (12) (2007) 4901–4910.
[17] Farhan Akram, Jeong Heon Kim, Kwang Nam Choi, Active contour method with locally computed signed pressure force function: an application to brain MR image segmentation, in: Seventh Int. Conf. Image Graphics, 2013, pp. 154–159.
[18] Yi-Ta Wu, Frank Y. Shih, Jiazheng Shi, Yih-Tyng Wu, A top-down region dividing approach for image segmentation, Pattern Recogn. 41 (2008) 1948–1960.
[19] Ayman El-Bazl, Aly A. Farag, Robert Falk, Renato La Rocca, Automatic identification of lung abnormalities in chest spiral CT scans, ICASSP (2003) 261–264.
[20] Jia Tong, Wei Yin, Wu Cheng Dong, A Lung cancer lesions detection scheme based on CT image, Int. Conf. Signal Process. Syst. (2010) 557–560.
[21] K. Martena, C. Engelke, T. Seyfarth, A. Grillhösl, S. Obenauer, E.J. Rummeny, Computer-aided detection of pulmonary nodules: influence of nodule characteristics on detection performance, Clin. Radiol. 60 (2005) 196–206.
[22] Zohreh Azimifar, Mohsen Keshani, Farshad Tajeripour, Reza Boostani, Lung nodule segmentation and recognition using SVM classifier and active contour modeling: a complete intelligent system, Comput. Biol. Med. 43 (2013) 287–300.
[23] Jamshid Dehmeshki, Hamdan Amin, ManlioValdivieso, Xujiong Ye, Segmentation of pulmonary nodules in thoracic CT scans: a region growing approach, IEEE Trans. Med. Imaging 27 (4) (2008) 467–480.
[24] Michael F. McNitt-Gray, Samuel G. Armato III, Charles R. Meyer, The lung image database consortium (LIDC) data collection process for nodule detection and annotation, Acad. Radiol. 14 (12) (2007) 1464–1474.
[25] Vicent Caselles, Ron Kimmel, Guillermo Sapiro, Geodesic active contours, Int. J. Comput. Vision 22 (1) (1997) 61–79.
[26] T. Chan, L. Vese, Active contours without edges, IEEE Trans. Image Process. 10 (2) (2001) 266–277.
[27] Li Wang, Lei He, Arabinda Mishra, Chunming Li, Active contours driven by local Gaussian distribution fitting energy, Signal Processing 89 (2009) 2435–2447.
[28] Chunming Li, Chiu-Yen Kao, John C. Gore, Zhaohua Ding, Implicit active contours driven by local binary fitting energy, in: IEEE Conf on Computer Vision and Pattern Recognition, 2007.
[29] Kaihua Zhang, Lei Zhang, Huihui Song, Wengang Zhou, Active contours with selective local or global segmentation: a new formulation and level set method, Image Vis. Comput. 28 (2010) 668–676.
[30] Chenyang Xu, Anthony Yezzi, JerryL Prince, On the relationship between parametric and geometric active contours, in: IEEE Proceedings, 2000.
[31] David S. Paik, Jiantao Pu, Justus Roos, Chin A. Yi, Sandy Napel, Geoffrey D. Rubin, Adaptive border marching algorithm: automatic lung segmentation on chest CT images, Comput. Med. Imaging Graphics 32 (2008) 452–462.
[32] D.S. Elizabeth, H.K. Nehemiah, C.S. Retmin Raj, A. Kannan, Computer-aided diagnosis of lung cancer based on analysis of the significant slice of chest computed tomography image, IET Image Process 6 (6) (2012) 697–705.
[33] Hao Han, Lihong Li, Fangfang Han, Bowen Song, William Moore, Zhengrong Liang, Fast and adaptive detection of pulmonary nodules in thoracic CT images using a hierarchical vector quantization scheme, IEEE J. Biomed. Health Infor. 19 (2) (2015) 648–659.
[34] Nor Amizam Jusoh, Jasni Mohamad Zain, Application of Freeman Chain Codes: an alternative recognition technique for Malaysian car plates, Int. J. Comput. Sci. Network Security 9 (11) (2009) 222–227.
[35] J.S.R. Jang, C.T. Sun, E. Mizutani, Neuro Fuzzy and Soft Computing, Pearson Education, Singapore, 2004.
[36] N.R. Pal, J.C. Bezdek, A mixed c-means clustering model, in: IEEE Int. Conf. Fuzzy Systems, 1997, pp. 11–21.
[37] H. Min, W. Jia, X.F. Wang, Y. Zhao, R.X. Hu, Y.T. Luo, F. Xue, An intensity-texture model based level set method for image segmentation, Pattern Recogn (2015).
[38] S.S. Kumar, R.S. Moni, J. Rajeesh, Automatic liver and lesion segmentation: a primary step in diagnosis of liver diseases, SIViP 7 (2013) 163–172.
[39] S. Hu, E.A. Hoffman, J.M. Reinhardt, Automatic lung segmentation for accurate quantitation of volumetric X-ray CT images, IEEE Trans. Med. Imaging 20 (6) (2001) 490–498.
[40] Y. Yim, H. Hong, Y.G. Shin, Hybrid lung segmentation in chest CT images for computer-aided diagnosis, in: IntWorkshop on Enterprise Networking and Computing in Healthcare Industry, 2005, pp. 378–383.
[41] P. Badura, E. Pietka, Soft computing approach to 3D lung nodule segmentation in CT, Comput. Biol. Med. 53 (2014) 230–243.
[42] G. Deep, L. Kaur, S. Gupta, Lung nodule segmentation in CT images using rotation invariant local binary pattern, ACEEE Int. J. Signal Image Process. 4 (1) (2013).